THE ASTROPHYSICAL JOURNAL, **293**:L59–L63, 1985 June 15

A RADIO AND OPTICAL STUDY OF A JET/CLOUD INTERACTION IN THE GALAXY CLUSTER A194[1]

JEAN P. BRODIE,[2,3] STUART BOWYER,[3] AND PATRICK MCCARTHY[2]
Department of Astronomy and Space Sciences Laboratory, University of California, Berkeley
Received 1985 January 11; accepted 1985 March 28

ABSTRACT

The cluster of galaxies Abell 194 has within it the strong radio source PKS 0123 − 016. Spectroscopic and photometric data we obtained in the field of this source have been combined with VLA maps to reveal a remarkable example of a jet/cloud interaction at the site of the peculiar galaxy known as Minkowski's object, which lies in the path of one of the radio jets discovered in this region. Our optical results can be used to rule out shock heating and power-law photoionization for this source and indicate a stellar origin for the ionizing flux. We therefore suggest that Minkowski's object was produced by a burst of star formation triggered by the impact of the jet on an obstructing cloud in its path.

Subject headings: galaxies: clustering — galaxies: jets — radio sources: galaxies

I. INTRODUCTION

Although extragalactic jets have long been known and are well studied in the radio, it has been only recently that promising theoretical models have been suggested for this phenomenon (Blandford and Königl 1979, and references therein). Even more recent is the use of optical techniques to study the interaction of these jets with their surrounding environment. This fruitful area of research was hampered by the difficulty of detecting intrinsically faint optical features against their relatively bright galaxy backgrounds. The advent of highly sensitive linear detectors has led to the discovery of optical emission in some, but by no means all, radio jets (for example, Heckman *et al.* 1982; Brodie, Königl, and Bowyer 1983; Brodie and Bowyer 1985; Simkin, Bicknell, and Bosma 1984; van Breugel *et al.* 1984, and additional papers by that group referenced therein). The number of radio jets surveyed is at present too small to allow reliable predictions of which jets will be emitting in the optical. However, tentative suggestions have been made connecting the presence of an optical jet to the radio spectral index (Butcher, van Breugel, and Miley 1980).

As part of a long-term program to investigate optical emission in jets, we have been studying the field of the double radio source PKS 0123 − 016 (3C 40). This strong radio source is situated near the center of the cluster Abell 194 and is particularly associated with the optical galaxies NGC 545 and 547. Embedded in a bridge of luminous material connecting NGC 545/547 to a nearby galaxy NGC 541 is a compact region (~ 10″ across) known as Minkowski's object (Minkowski 1958) and referred to by Simkin (1976) as a peculiar galaxy. Its redshift was measured by Simkin as ~ 0.019 confirming its association with Abell 194. She reported blue *UBV* colors and high-excitation emission lines and other spectral properties suggestive of the type of activity seen in strong radio galaxies.

Our study of this source began with a radio mapping of the entire region using the VLA, followed by deep imaging and spectroscopy in the optical. The combination of our radio and optical images is clearly suggestive of a jet/cloud interaction. We describe these images and our spectroscopic results in § II. In § III, we suggest a general picture for the formation of Minkowski's object and the excitation mechanisms involved. Our results are summarized in § IV.

II. OBSERVATIONS

The radio source PKS 0123 − 016 was observed in 1983 April at 20 cm with the VLA in C configuration. The data were reduced using standard procedures with the on-site VLA reduction software and employing the CLEAN algorithm to produce the radio maps shown in Figure 1. The position of Minkowski's object is indicated by the hatched area. Note that Minkowski's object lies in a region of low radio polarization.

The optical follow-up was conducted in two phases comprising direct imaging and spectroscopy of the Abell 194 field. Direct images were obtained using the PFCCD on the 4 m telescope at CTIO and the Cassegrain CCD on the 3 m at Lick Observatory. The optical data were reduced using the standard software packages at CTIO and using the Lick data reduction software available on the Berkeley VAX system. The Lick CCD image of the field is shown in Figure 2 (Plate L2). The positions of two emission regions or "knots" are indicated. These condensations lie within a main ridge of enhanced emission. In Figure 3 (Plate L3) we superpose the optical and the VLA radio maps. Our CCD images provided $B - V$ colors and V magnitudes which were linearly related to

[1] Based in part on observations at Lick Observatory.

[2] Visiting Astronomer, Cerro Tololo Inter-American Observatory, operated by AURA, Inc., under contract with the National Science Foundation.

[3] Visiting Astronomer, National Radio Astronomy Observatory (VLA), operated by Associated Universities, Inc., under contract with the National Science Foundation.

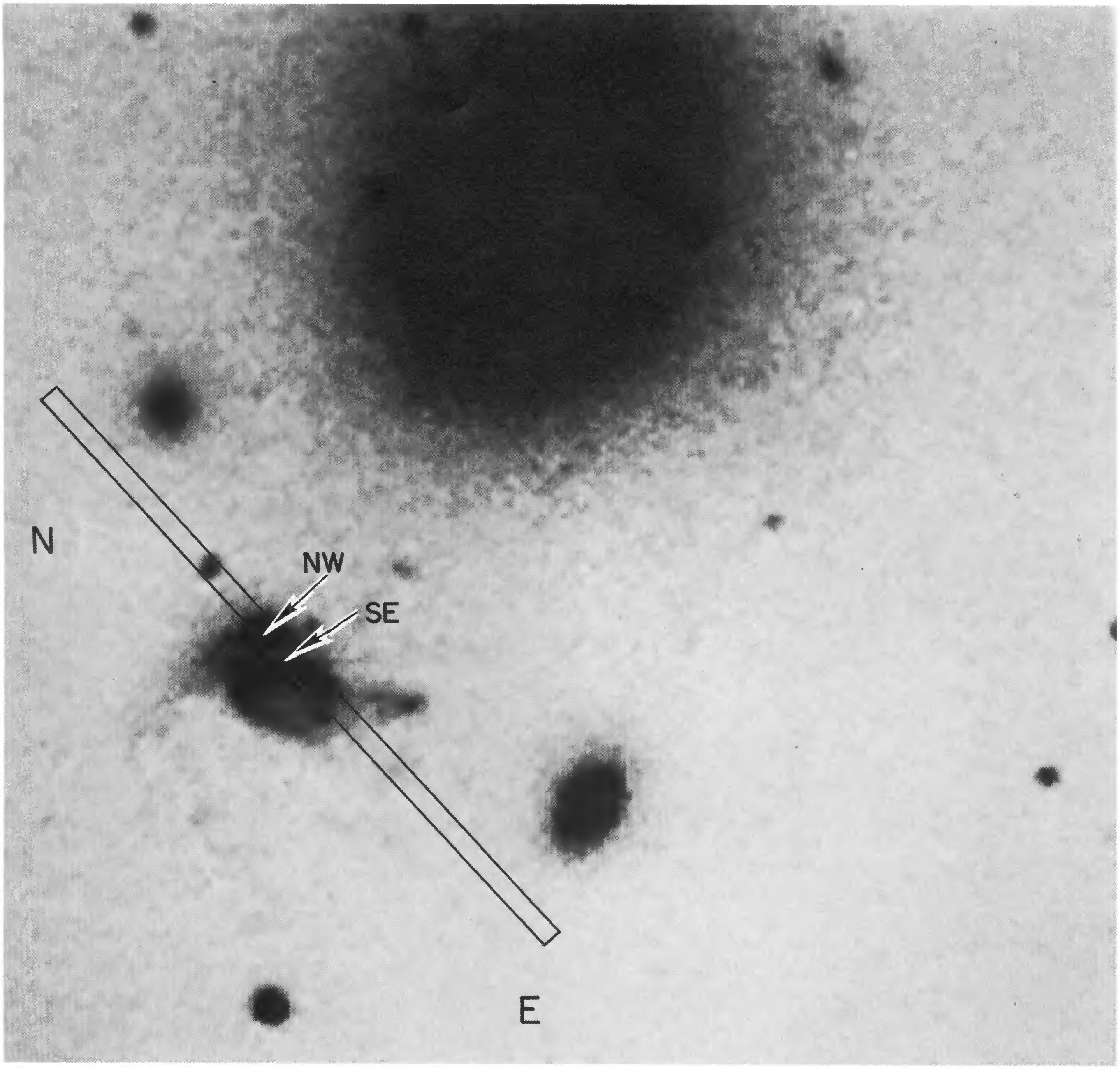

FIG. 2.—CCD image of the field of PKS 0123−016. The NW and SE knots are indicated as is the primary slit position used for the spectroscopic study. The bandpass of the image is 6000–7200 Å.

BRODIE, BOWYER, AND MCCARTHY (*see* page L59)

1985ApJ...293L..59B

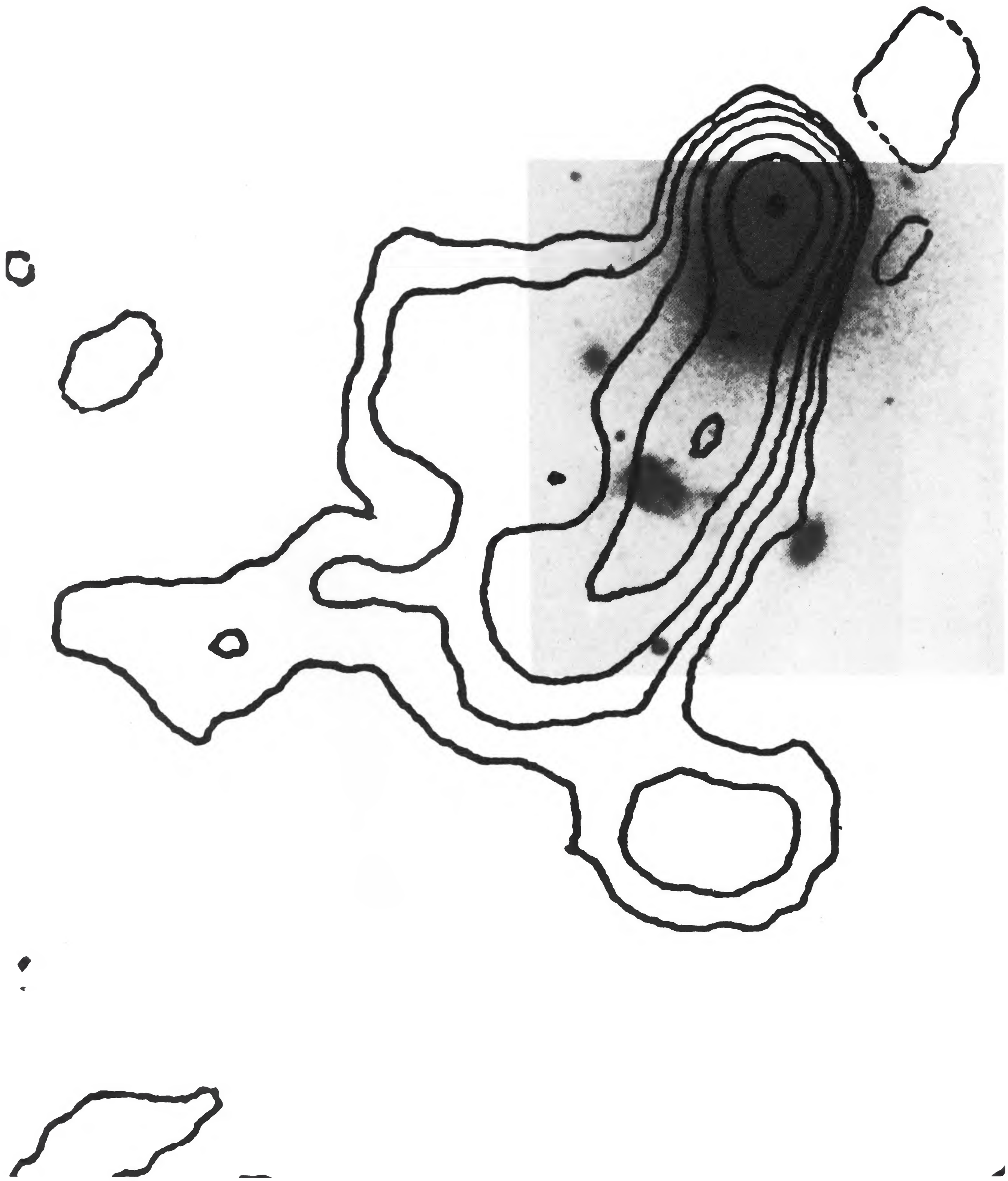

FIG. 3.—The superposition of the VLA radio map with the CCD optical image

BRODIE, BOWYER, AND MCCARTHY (*see* page L59)

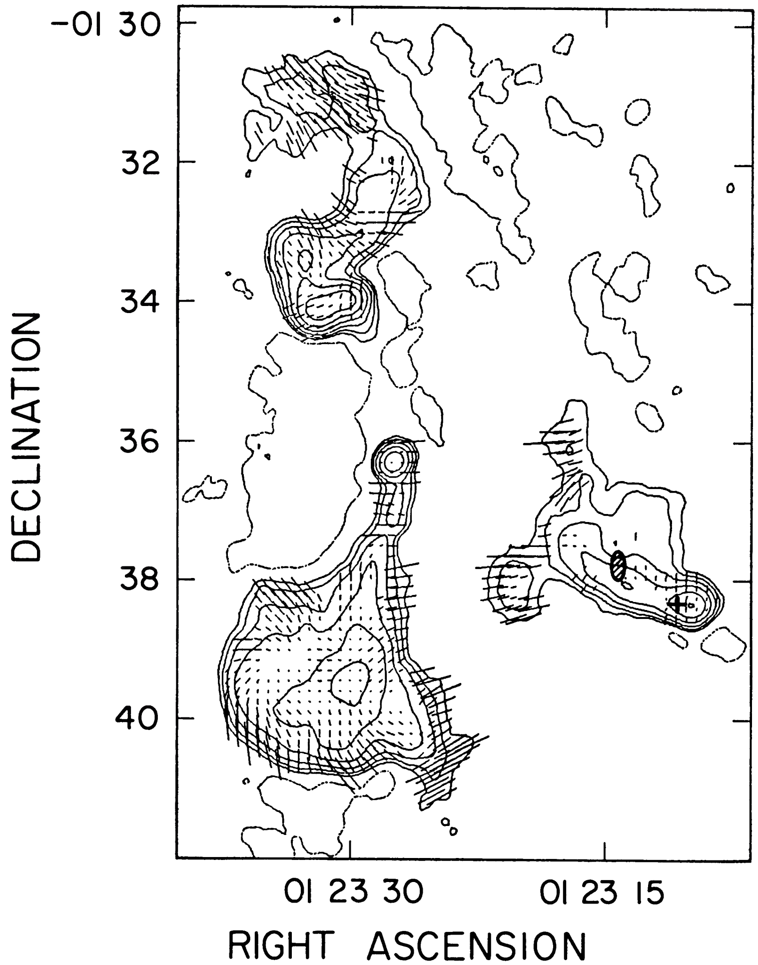

FIG. 1.—VLA map of the field of PKS 0123−016 obtained at 20 cm in C configuration. Vectors indicate the strength and direction of the radio polarization. The peak flux is 1.1155E − 01 Jy per beam. The position of Minkowski's object is indicated by a hatched area, and the nucleus of NGC 541 is marked by +.

two standard stars observed before and after the observations of Minkowski's object. The absolute photometry is therefore somewhat crude; however, these magnitudes provide a reliable gauge of relative color for objects in the field. For the object as a whole we find $V = 17.24$ and $(B - V) = -0.19$, in reasonably good agreement with the photometric results of Simkin (1976). The deep CCD images show extensive diffuse filamentary structure downstream of the emission ridge, indicating a disruption of the object. The relatively bright ridge of emission perpendicular to the main emission ridge is suggestive of complex interaction between the gas and the jet, especially since both of these ridges are somewhat bluer than the rest of the object. We note the presence of two small regions of enhanced emission whose positions lie in a line between Minkowski's object and the edge of the nucleus of the nearby galaxy NGC 541. This line coincides with the brightest part of the radio jet emanating from this elliptical galaxy.

Spectroscopy was carried out using the Lick CCD in long-slit mode on the 3 m telescope and on the 4 m telescope at CTIO with the SIT Vidicon detector, also in long-slit mode. The total wavelength range covered by these spectra was 4200–7000 Å with resolutions from 3 to 10 Å. A sample spectrum of Minkowski's object obtained at the slit position marked in Figure 2 is shown in Figure 4. Spectra of the southeast knot and the main emission ridge as a whole were also obtained. We see no evidence for absorption features in the continuum which implies that the contribution from late-type stars must be small. SIT Vidicon spectral data we obtained of the other main radio jet in the A194 system which lies south of the NGC 545/547 galaxy pair showed no regions of enhanced optical emission associated with that radio jet.

In Table 1 we give the line strengths measured from spectra obtained at Lick Observatory using a CCD and a 600 lines mm^{-1} grism with a wavelength coverage of 4200–6900 Å at ~ 10 Å resolution, and a CCD and one order of a high-resolution eschism with a wavelength coverage of 6200–7000 Å at ~ 3 Å resolution. Line strengths are provided for the southeast knot, the northwest knot, and the region between the knots. Also shown are integrated line strengths for the main ridge of emission as a whole. The focus was found to vary across the face of the CCD chip and was optimized for the center of the wavelength coverage. This caused lines near the extremes of the wavelength range to appear with degraded resolution. For this reason, the high-

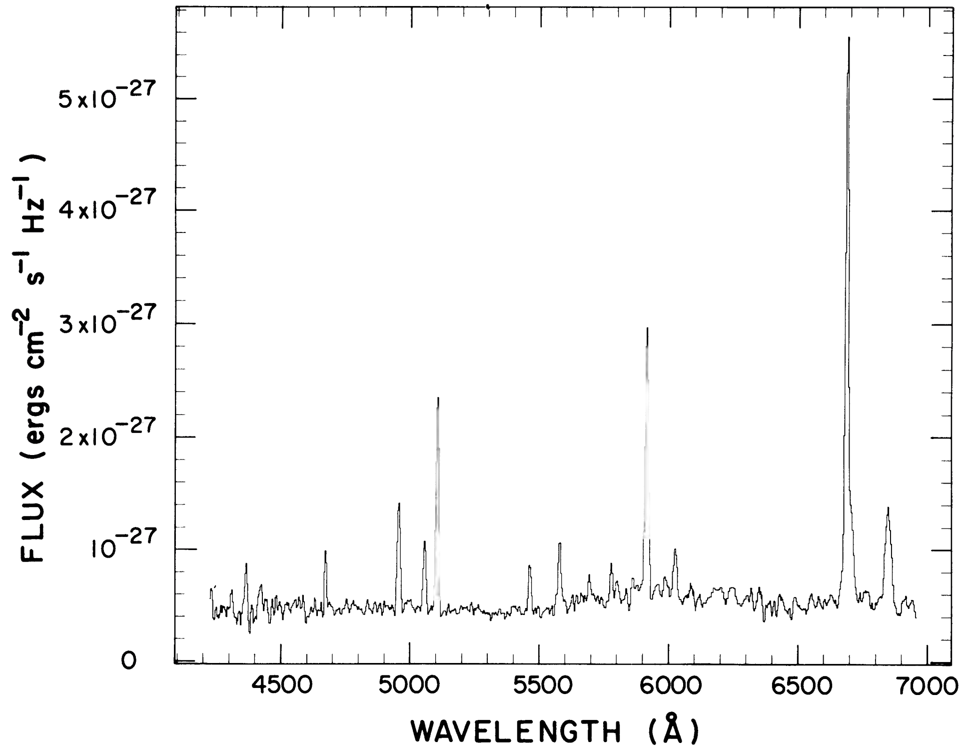

FIG. 4.—A sample spectrum of Minkowski's object obtained at the slit position marked on Fig. 2. The spectrum was obtained using a 600 lines mm^{-1} grism and covers the bandpass 4200–7000 Å.

resolution eschism data were used to determine the ratio of [S II] 6717 to [S II] 6731. However, the strength of the [S II] doublet was established from the 600 lines mm^{-1} grism spectra, as sky subtraction was best achieved with the lower resolution data. We interpret the steep Balmer decrement as due to reddening. A reddening correction can be estimated from the observed value of the Balmer decrement, assuming an intrinsic value of $H\alpha/H\beta = 2.86$ (Osterbrock 1974). However, $H\beta$ is beyond the range covered by the high-resolution eschism data and $H\alpha$ is blended with [N II] 6584 in the lower resolution 600 lines mm^{-1} grism data. In order to determine an observed value of $H\alpha/H\beta$, for comparison with the intrinsic value, we used the eschism data to establish the percentage of the $H\alpha$, [N II] blend which can be attributed to $H\alpha$. In both the SE and the NW knots, $H\alpha$ contributes $\sim$ 91% of the total $H\alpha$, [N II] line flux. By removing the contribution of [N II] from the blended line we were able to determine the $H\alpha/H\beta$ ratios for both knots from the 600 lines mm^{-1} grism spectra. Reddening-corrected line strengths are given in Table 1.

We estimate that the error in the line strengths ranges from 5% to 15% for the strongest and weakest lines, respectively. This is derived from an assessment of the signal-to-noise ratio (S/N) of the spectra, judged partly by the strength of the smallest measurable feature, and from the range of line strengths obtained using a variety of acceptable fits to the local continuum. The error involved in fitting the continuum (1%–8%) is dominated by S/N errors. The particularly weak lines $H\gamma$ and [O III] λ4363 are marked with a colon in Table 1. Further uncertainties, especially in the Balmer line strengths, arise if the continuum is dominated by young hot stars. The strengths of Balmer absorption features due to a population of young stars are difficult to estimate as they depend on a variety of factors such as age and the exact population mix.

III. DISCUSSION

The presence of an optically emitting condensation in the path of a radio jet is clearly suggestive of a jet/cloud interaction. Three possible mechanisms can give rise to optical line emission in the gas associated with such an object: shock heating, photoionization by nonthermal continuum radiation, or photoionization by starlight. Shocks can result from the impact of the jet with dense material in its path. These may excite the gas directly or produce continuum radiation which in turn photoionizes the gas (see Brodie, Königl, and Bowyer 1983 for further discussion of these alternatives). An alternative source of photoionizing flux is the same synchrotron process which is responsible for the observed radio emission. If, however, the optical emission is the result of recent star formation, perhaps triggered by the impact of the jet on protostellar material, the optical spectrum of Minkowski's object should resemble an H II region and should display line strength ratios significantly different from such shock-excited or power-law photoionized sources.

The results of Simkin (1976) argue against a stellar interpretation as she reported the presence of high-excitation lines ([Ne V] and He II), a steep Balmer decrement, and line strength ratios ([S II] λ6717/λ6731; [O III] λ(4959+5007)/λ4363) indicative of electron densities and temper-

TABLE 1

LINE STRENGTHS FOR MINKOWSKI'S OBJECT

	SE KNOT (2″ × 3″.5)				NW KNOT (2″ × 3″.5)				INTEGRATED RIDGE (2″ × 10″.5)			
	600 Lines mm^{-1}		Eschism		600 Lines mm^{-1}		Eschism		600 Lines mm^{-1}		Eschism	
λ Å	Raw Relative to Hα = 100	Reddening Corrected	Raw Relative to Hα = 100	Reddening Corrected	Raw Relative to Hα = 100	Reddening Corrected	Raw Relative to Hα = 100	Reddening Corrected	Raw Relative to Hα = 100	Reddening Corrected	Raw Relative to Hα = 100	Reddening Corrected
Hγ 4340	...	...	...	...	...	...	...	...	7.6:	9.6	...	...
[O III] 4363	...	...	...	...	...	...	...	...	2.5:	3.2	...	...
He II 4686	...	...	...	...	...	...	...	...	< 1.8	...	...	...
Hβ 4861	26.3	34.9	...	...	24.9	35.0	...	...	29.6	35.0	...	...
[O III] 4959	18.0	23.2	...	...	25.2	34.1	...	...	24.1	27.9	...	...
[O III] 5007	60.3	77.6	...	...	76.7	103.7	...	...	77.5	89.8	...	...
[O I] 6300	...	...	...	...	...	...	...	...	< 1.8	...	...	...
Hα 6563	100.0[a]	100.0	100.0[b]	100.0	100.0[c]	100.0	100.0[d]	100.0	100.0[e]	100.0	100.0[f]	100.0
[N II] 6584	9.1	9.1	9.1	9.1	9.9	9.9	9.9	9.9	10.2	10.2	10.2	10.2
[S II] 6717 } [S II] 6731 }	20.0	19.6	12.4	12.1	23.4	22.9	13.8	13.5	23.5	23.3	13.4	13.2
			7.6	7.5			9.6	9.4			10.1	10.0
Ratios												
Hα/Hβ	3.80	2.86	...	...	4.02	2.86	...	...	3.38	2.86	...	...
[N II] 6584/Hα	...	...	0.09	...	...	...	0.10	...	...	...	0.10	...
[S II] 6717/6731	...	...	1.62	...	...	...	1.43	...	...	...	1.32	...

[a] $H\alpha = 0.619 \times 10^{-14}$ ergs s^{-1}.
[b] $H\alpha = 0.759 \times 10^{-14}$ ergs s^{-1}.
[c] $H\alpha = 0.595 \times 10^{-14}$ ergs s^{-1}.
[d] $H\alpha = 0.563 \times 10^{-14}$ ergs s^{-1}.
[e] $H\alpha = 1.573 \times 10^{-14}$ ergs s^{-1}.
[f] $H\alpha = 1.834 \times 10^{-14}$ ergs s^{-1}.

atures significantly higher than is typical for H II regions. However, we have subjected our data to the line strength classification scheme of Baldwin, Phillips, and Terlevich (1980) which has been widely used to distinguish between H II regions, objects photoionized by a power-law continuum, and objects which have been shock heated. We find that Minkowski's object lies in the area dominated by H II regions. We see no evidence for the high-excitation line of He II reported by Simkin down to a sensitivity limit of 0.94×10^{-16} ergs s^{-1} in each knot. We cannot comment on the presence or absence of the [Ne V] line which she detected as it is beyond our spectral coverage.

Considering the available data as a whole, the excitation mechanism responsible for Minkowski's object remains a puzzle. However, if we confine ourselves only to our own data, we may be able to exclude shock heating and power-law photoionization as possible excitation mechanisms. Our data allow us to place a much more stringent limit on the presence of [O I] λ6300 than was obtained by Simkin. We find no evidence for [O I] λ6300 emission down to our sensitivity limit. We note that the λ6300 Å line is strong in objects excited by shock heating or photoionized by a power-law continuum (Baldwin, Phillips, and Terlevich 1980; Ferland and Netzer 1983), and this line is typically weak or absent in H II regions, independent of their metallicity. Moreover, the ratio of [N II] λ6584/Hα λ6563 we obtain is much smaller than we would expect from shock-excited sources.

Other characteristics are more ambiguous. In principle, temperature is a powerful discriminator between shock heating and photoionization, and it can be determined from a measurement of the [O III] ratio (λ4959+λ5007)/(λ4363) (Osterbrock 1974). As [O III] λ4363 is a weak line we measured its strength from a spectrum which combined the light from the entire emission ridge in order to improve the S/N. Combining this with our values of λ4959 and λ5007 for the ridge area we find, after correcting for reddening, [O III] (λ4959+λ5007)/λ4363 ≈ 37, which implies an electron temperature in excess of 20,000 K. This is very high for normal H II regions, whose temperature is typically 8,000–10,000 K (Osterbrock 1974). However, the uncertainties involved in measuring the λ4363 line, its intrinsic weakness and the proximity of Hγ, suggest that this discrepancy may not be a serious one, although temperatures above 20,000 K are certainly more typical of shocks. The theoretical power-law photoionization models of Ferland and Netzer (1983) predict little λ4363 emission, and therefore low temperatures, so that taken at face value, the derived temperature indicates shock excitation. A possible explanation may be that we are observing the effects of a combination of shock heating and photoionization by starlight. The [O III] lines at least may be formed in a shock-heated region, and we note that the ridge morphology within the source is very suggestive of a shock. The densities we derive from the [S II] λ6717/λ6731 ratio (Osterbrock 1974) are between 10 and 50 cm^{-3} for the knots and 170

cm^{-3} for the whole ridge, provided the electron temperature is in the region of 10^4 K, although the derived density is not particularly sensitive to the assumed temperature. Within the uncertainties it appears that the northwest knot has a slightly higher density than the southeast knot. (Other small differences in line strengths are apparent between the knots though there is no perceptible velocity shift between them.) These low densities are entirely consistent with normal H II regions (Osterbrock 1974) though they are also consistent with shock-excited objects. For example, the shock models of Shull and McKee (1979), which refer to shock velocities between 40 and 130 km s^{-1}, predict values for the [S II] ratio ranging between 0.68 and 1.45. Adopting the mean ridge value of 170 cm^{-3} as representative of the source as a whole and using our measurements of the Hα luminosity we can estimate the mass of optically emitting gas in Minkowski's object as $\sim 10^5\ M_{\odot}$.

On the basis of a purely empirical comparison with published data on H II regions we find that the integrated strength of the [S II] doublet is high for a metal-poor H II region (French 1980; Knuth and Sargent 1983), although it is in closer agreement with metal-rich H II regions (of about 60% solar abundance) than with shock models. However, this argument may be weakened due to the contamination of the [S II] lines by the presence of airglow at this wavelength. A high metal abundance is certainly hard to reconcile with the high temperatures indicated by the [O III] line measurements, if the object is photoionized by starlight. In fact, such high temperatures can only be sustained in a source so extremely metal deficient that cooling is inhibited. Since the measurements of both [O III] and the [S II] doublet strength are uncertain, errors in one or both may be producing this discrepancy. The [N II]/Hα ratio agrees better with metal-rich H II regions than metal-poor ones and is very different from shock models. Power-law ionization models such as those described by Ferland and Netzer (1983) can be made to reproduce a low value for the [N II]/Hα ratio as well as strong [S II] by adjusting the metal abundance and/or the ionization parameter. Nonetheless, the absence of [O I] λ6300 is a strong argument against power-law photoionization of this source. Similarly, the unequivocal absence of λ6300 is the key piece of evidence which allows us to reject a shock model.

The following general conclusions may be drawn from our observations. Our spectroscopic data indicate a stellar origin for the ionizing flux; the blue color of Minkowski's object and the absence of absorption features in the spectrum require that the stellar population be young. The continuum radiation from the object is extremely flat over the wavelength range 3700–7000 Å with typical flux levels of 5×10^{-28} ergs cm^{-2} s^{-1} Hz^{-1}. The extrapolation of this continuum to shorter wavelengths is therefore more than sufficient to photoionize the gas. The activity within the object, which is accentuated by the presence of diffuse filamentary structure downstream of the main emission ridge, indicates that the source and the jet are physically interacting. The simplest interpretation of the data is that an interstellar cloud, possibly comprising preenriched gaseous material, is swept into the path of the jet streaming from the nucleus of NGC 541. Enrichment of the interstellar material within the cluster of galaxies is not unexpected, given the preferential aggregation of processed material toward the center of a cluster's gravitational potential well. The impact of the jet on the gaseous cloud could then trigger a burst of star formation while simultaneously initiating a disruption of the cloud.

We gratefully acknowledge the help of Remington Stone in acquiring the optical data and John Clarke, Chris O'Dea, and Rick Perley in acquiring the radio data. This work was supported by NSF grant AST-8005874-A01 and the UK Science and Engineering Research Council.

Note added in manuscript.—Subsequent to the submission of this manuscript, van Breugel, in a later paper at the 1985 January meeting of the American Astronomical Society, presented data on this object which, though differing in detail, are in overall agreement with the data presented here.

REFERENCES

Baldwin, J., Phillips, M., and Terlevich, R. 1980, *Pub. A.S.P.*, **93**, 5.
Blandford, R. D., and Königl, A. 1979, *Ap. J.*, **232**, 34.
Brodie, J., and Bowyer, S. 1985, *Ap. J.*, **292**, 447.
Brodie, J., Königl, A., and Bowyer, S. 1983, *Ap. J.*, **273**, 154.
Butcher, H., van Breugel, W. J. M., and Miley, G. K. 1980, *Ap. J.*, **235**, 749.
Ferland, G. J., and Netzer, H. 1983, *Ap. J.*, **264**, 105.
French, H. B. 1980, *Ap. J.*, **240**, 41.
Heckman, T. M., Miley, G. K., Balick, B., van Breugel, W. J. M., and Butcher, H. R. 1982, *Ap. J.*, **262**, 529.
Knuth, D., and Sargent, W. L. W. 1981, *Ap. J.*, **273**, 81.
Minkowski, R. 1958, *Pub. A.S.P.*, **70**, 143.
Osterbrock, D. E. 1974, *Astrophysics of Gaseous Nebulae* (San Francisco: Freeman), p. 69.
Shull, J. M., and McKee, C. F. 1979, *Ap. J.*, **227**, 131.
Simkin, S. M. 1976, *Ap. J.*, **204**, 251.
Simkin, S. M., Bicknell, G. V., and Bosma, A. 1984, *Ap. J.*, **277**, 513.
van Breugel, W. J. M., Heckman, T. M., Butcher, H. R., and Miley, G. K. 1984, *Ap. J.*, **276**, 79.

STUART BOWYER and PATRICK MCCARTHY: Department of Astronomy, University of California, Berkeley, CA 94720

JEAN P. BRODIE: Space Sciences Laboratory, University of California, Berkeley, CA 94720